Published in final edited form as:
Neuroimage. 2010 March ; 50(1): 7. doi:10.1016/j.neuroimage.2009.12.053.

Temporary Disruption of the Rat Blood-Brain Barrier with a Monoclonal Antibody: A Novel Method for Dynamic Manganese-Enhanced MRI

Hanbing Lu, **Steven Demny**, **Yantao Zuo**, **William Rea**, **Leiming Wang**, **Svetlana I. Chefer**, **D. Bruce Vaupel**, **Yihong Yang**, and **Elliot A. Stein**
Neuroimaging Research Branch, National Institute on Drug Abuse, National Institutes of Health, Baltimore, MD 21224

Abstract

Manganese (Mn^{2+}) has limited permeability through the blood-brain barrier (BBB). Opening the BBB such that a sufficient amount of Mn^{2+} enters the extracellular space is a critical step for dynamic manganese-enhanced magnetic resonance imaging (ME-MRI) experiments. The traditional BBB opening method uses intracarotid hyperosmolar stress which results in suboptimal BBB opening, and practically is limited to nonsurvival experiments due to substantial surgical trauma. In the present ME-MRI study, we investigate the feasibility of opening the BBB with an antibody that targets the endothelial barrier antigen (EBA) specifically expressed by rat endothelial cells. Results demonstrate that intravenous infusion of the anti-EBA agent SMI-71 leads to BBB disruption of the whole brain as detected by ME-MRI and confirmed by Evans blue dye staining. Physiologically, injection of SMI-71 leads to a hypertensive response followed by a sustained hypotensive response in animals anesthetized with urethane alone. Incorporating isoflurane partially mitigated both pressor responses. In general, BBB disruption via intravenous infusion of SMI-71 is straightforward and obviates technical difficulties associated with intracarotid hyperosmolar stress, opening new possibilities for *in-vivo* neuroimaging with ME-MRI. The data also suggest that ME-MRI may be used as an imaging method to assess BBB integrity complementary to the Evans blue dye method, a classical but highly invasive technique, permitting longitudinal assessment of the integrity of the BBB on the same animal.

Keywords

blood-brain barrier; manganese-enhanced MRI; endothelial barrier antigen; mannitol; manganese

Introduction

Manganese-enhanced magnetic resonance imaging (ME-MRI) has rapidly evolved into a promising neuroimaging tool. Mn^{2+} can be transported anterogradely, permitting *in-vivo* neuronal tract tracing (Canals et al., 2008; Pautler et al., 1998; Watanabe et al., 2006). In addition to its neuroanatomical applications, functional studies can be performed by taking

Correspondence should be addressed to: Elliot A. Stein, Ph.D., Neuroimaging Research Branch, National Institute on Drug Abuse, NIH, 251 Bayview Blvd., Suite 200, Rm. 7A711, Baltimore, MD 21224, Tel: (443) 740-2650, estein@intra.nida.nih.gov.

advantage of the fact that Mn^{2+} is a Ca^{2+} analogue and can be taken up by neuronal cells through voltage-gated or ligand-gated Ca^{2+} channels. The resulting ME-MRI signal reflects active synaptic transmission, obviating the hemodynamic transduction process and vascular dynamics most commonly employed in functional MRI studies. This functional ME-MRI technique has been successfully applied to map neuronal response to somatosensory stimulation (Aoki et al., 2002; Duong et al., 2000), olfactory bulb activity to odor stimulation (Pautler et al., 2002), hypothalamic function associated with feeding (Kuo et al., 2006), midbrain response to auditory stimulation (Yu et al., 2005, 2007) and neuronal activity following drug challenge (Hsu et al., 2008, Lu et al., 2007).

However, the blood-brain barrier (BBB) has very low permeability to Mn^{2+} (Fitsanakis et al., 2005), raising potentially significant methodological limitations. For studies focusing on structures that have limited BBB, such as olfactory tubercle, superior colliculus, and hypothalamus (Kolb and Whishaw, 2003), functional ME-MRI studies can be performed following systemic administration of Mn^{2+}. For studies employing manipulations that would be expected to have more system-wide effects, such as drug administrations where multiple cortical and subcortical structures are expected to be activated, temporary disruption of the BBB appears to be necessary for whole brain imaging. BBB disruption through hyperosmolar challenge (Beck et al., 1984), as used in a pioneering ME-MRI experiment (Lin and Koretsky, 1997), requires catheterization of the carotid artery to permit a bolus injection of hyperosmolar mannitol to the internal carotid artery. The mannitol bolus is then distributed to the anterior, middle, and posterior cerebral arteries via the circle of Willis. Various factors, including the amount of mannitol, the speed and duration of the injection, and the temperature of the drug solution can influence the extent of BBB disruption (Aoki et al., 2004; Gumerlock et al., 1990); those brain areas with intact BBB will have negligible Mn^{2+} accumulation into activated neurons, leading to a false-negative outcome in functional ME-MRI experiments. Furthermore, carotid artery catheterization effectively limits this technique to non-survival experiments due to substantial residual surgical trauma. To date, suboptimal BBB opening remains a technical bottleneck for functional ME-MRI studies, motivating the search for better methods to overcome the above-mentioned technical difficulties.

The endothelial barrier antigen (EBA) is a protein selectively and specifically expressed by endothelial cells of the rat BBB, although its exact function is not known. A previous study (Sternberger and Sternberger, 1987) showed that EBA could be detected by tissue immunostaining using a monoclonal antibody, which can be used to identify the BBB in-vitro. A study by Ghabriel et al. (2000) suggested that immunological targeting of the EBA by intravenous administration of a monoclonal antibody (anti-EBA) leads to acute BBB opening to exogenous and endogenous tracers. This BBB opening method avoids traumatic surgical preparation and provides a potentially novel Mn^{2+} delivery method to the entire central nervous system for whole brain ME-MRI functional imaging.

In the present study, we evaluated the feasibility of using an anti-EBA agent to facilitate ME-MRI experiments. Studies were performed with different anesthesia protocols and anti-EBA agent doses. Results demonstrate that the ME-MRI signal was significantly enhanced in many cortical and subcortical structures following anti-EBA administration, indicating acute BBB disruption and opening new possibilities for *in-vivo* neuroimaging using Mn^{2+} as a contrast agent. A preliminary account of this work has been presented in abstract form (Lu et al., 2009).

Methods

Bench Experiments

A previous study (Gumerlock et al., 1990) revealed that the choice of anesthetic agents affected the outcome of BBB disruption via hyperosmolar stress. To determine the proper anesthetics for the current experiment, we performed non-imaging studies to test three types of anesthetic agents that are commonly used in MRI: urethane (1.2 g/kg I.P.), isoflurane (1.8% in oxygen enriched air) and α-chloralose (80 mg/kg loading dose followed by 50 mg/kg I.V. constant infusion). Animals were assigned into three experimental groups according to the anesthetics they received, with 4-5 rats in each group. An anti-EBA agent (SMI-71) in vehicle (HA.11) (both from Innovative Antibodies, CA, USA) was infused intravenously (30 μl in 0.4 ml saline) over 5 min. The dose and infusion rate were chosen based on a previous report (Ghabriel et al., 2000). Five minutes after SMI-71 infusion was finished, 2% Evans blue dye (Sigma Chemical) was injected intravenously (3ml/kg). Five minutes later, animals were decapitated and the brain was harvested and grossly dissected. Evans blue dye binds to serum albumin, giving rise to a high-molecular complex. It remains intravascular and diffuses to extra-vascular space only following BBB disruption (Wolman et al., 1981), which was evaluated by examining the color of the brain sections by at least two independent observers. Of the three anesthetic agents examined, animals anesthetized under urethane gave the most consistent BBB disruption outcome, and was chosen as the anesthetic agent for subsequent imaging experiments. In addition, to determine the optimum dose for BBB disruption, in preliminary studies, SMI-71 was also administered at 25 μl (n=6) and 20 μl (n=4).

Animal Preparation for Imaging Study

Sprague-Dawley rats weighing 250-350g were anesthetized with urethane (1.2 g/kg, I.P.), a double-lumen catheter was inserted into a femoral vein for drug delivery, and a femoral artery was catheterized for blood pressure monitoring and blood gas sampling. Rats were intubated for artificial ventilation (SAR-830 ventilator; CWE, Ardmore, PA) and for administering isoflurane as described below. A neuromuscular blocking agent (Pancuronium Bromide, Sicor Pharmaceuticals, Inc., Irvine, CA) was administered (I.V.) with a loading dose of 2.0 mg/kg followed by a constant infusion of 2.0 mg/kg/hr (Harvard Apparatus, Holliston, MA). Animals were secured via a customized head holder with bite bar and ear bars and positioned within the center of the magnet. End-tidal CO_2 and O_2 were continuously monitored (GEMINI Respiratory Gas Analyzer, CWE, Ardmore, PA) and core body temperature was maintained at 37.0 ± 1.0°C with a water-circulating bed. After the experiments, all rats were euthanized by overdose pentobarbital (100 mg/kg I.V.).

Imaging Protocol

The imaging protocol was similar to that in our previous report (Lu et al., 2007). Specifically, ten minutes of baseline images were acquired following anatomical localization scans. Constant I.V. infusion of 1% $MnCl_2$ in saline (Sigma, St. Louis, MO) was subsequently initiated using an infusion pump (Harvard Apparatus, Holliston, MA) with an infusion rate of 20 mg/kg/hr, lasting for twenty minutes. SMI-71 (30 μl) was diluted into 0.4 ml saline and infused (I.V.) over five minutes with an infusion pump. Once SMI-71 infusion was complete, $MnCl_2$ infusion was resumed while T_1-weighted images were continuously acquired for 50~200 min depending upon experimental requirements. Rats were divided into four experimental groups. The first group (n=10) received SMI-71 (30 μl in 0.4 ml saline) under urethane anesthesia. The second group (n=6) received the same amount of vehicle and served as a control. Because SMI-71 led to a dramatic and immediate blood pressure increase followed by a sustained hypotensive response in the first group (see Fig. 5 in the results section), a third group of urethane anesthetized rats (n=6) received the same amount of SMI-71 (30 μl) while isoflurane (1.8~2.2%) was administered 10 min prior to and 15 min after SMI-71

administration to mitigate the dramatic blood pressure changes utilizing isoflurane's vasodilatory effects (Jensen et al., 1992). In order to compare the effect of infusion rate on BBB disruption and blood pressure, in group four (n=4), the infusion duration was increased from 5 min to 10 min, while keeping the amount of SMI-71 constant. To determine if the rat BBB is indeed disrupted under urethane+isoflurane anesthesia with an SMI-71 dose of 30 μl, we repeated the Evans blue dye experiments on 6 animals (n=4 for SMI-71, n=2 for vehicle) except that Evans blue dye was injected 40 min after the animals had received SMI-71 or vehicle. Brain tissue was cut into 2 mm thick slices using a rat brain matrix and was then subject to visual examination under a microscope.

To assess potential pathological effects of the agents (SMI-71 and the vehicle) to vital organs, nine animals received three different treatments (n=5 for SMI-71, n=2 for vehicle and n=2 for saline) and were continuously scanned for 2.5 hours, during which the $MnCl_2$ infusion pump was alternatively turned on and off for 30 min periods. Kidney, heart and lung tissues were harvested from each animal at the end of the experiments and were subject to pathological examination. Two additional animals were scanned without harvesting the tissues. The resulting ME-MRI data were also used to determine how long the BBB remained open once it was disrupted. All experimental procedures were approved by the Animal Care and Use Committee at the National Institute on Drug Abuse, NIH.

Data Acquisition

MRI experiments were performed on a Bruker Biospin 9.4T scanner (Bruker, Karlsruhe, Germany) equipped with an actively shielded gradient coil. The inner diameter of the gradient coil was 12 cm, and the maximum gradient strength was 40 mT/m. A birdcage coil driven in linear mode was used for RF excitation, and a single-turn circular surface coil (2.5 cm in diameter) was used for signal reception. For slice localization and image registration, high-resolution T_2-weighted anatomical images were acquired using a rapid acquisition with relaxation enhancement (RARE) sequence: repetition time (TR) = 2650 ms, effective echo time (TE) = 50 ms, RARE factor = 8. The total number of slices was 23, slice thickness = 1 mm. The anterior commissure was used as a reference point for image acquisition, which approximately corresponds to -0.36 mm from bregma (Paxinos and Watson, 2005). Since Mn^{2+} is known to shorten tissue T_1 values, ME-MRI signal is detected with a T_1-weighted conventional spin echo sequence. Scan parameters were: TR/TE = 450/8 ms, slice thickness = 1 mm, spectral width = 50 kHz, field of view = 3.5 cm, matrix size = 128 × 128, number of slices = 13. A customized program (Lu et al., 2008) was developed to receive k-space data, reconstruct images and display voxel-wise time courses in a realtime fashion within the Analysis of Functional NeuroImages (AFNI) framework (Cox, 1996). The results of BBB disruption following anti-EBA agent injection were readily evident using this method.

Data Analysis

To facilitate group comparisons, images from each animal were manually registered onto a common 3D space within the AFNI framework (Cox, 1996) using the method previously described (Lu et al., 2007). Briefly, T_2-weighted images from one animal that had the best positioning were selected as a template. Ten prominent anatomical reference points were identified from this template and subsequently identified in each set of structural images to be registered. A transformation matrix including linear transformation and rotational elements was generated by minimizing the errors of the coordinates of the anatomical reference points using a least-squares approach. This transformation matrix was subsequently applied to the dataset acquired during the ME-MRI scans.

The effect of SMI-71 on BBB integrity was evaluated by computing the fractional signal enhancement relative to pre-SMI-71 baseline. Specifically, data points before SMI-71 infusion

(S_0) and data points at the end of SMI-71 infusion (S_1) were calculated, this was done by averaging three neighboring data points pre- and at the end of SMI-71 scans, respectively. Fractional signal change relative to pre-SMI baseline was calculated on a voxel-wise basis using the formula: $100\times(S_1-S_0)/S_0$. Statistical comparisons of ME-MRI signal changes between the three treatment groups (urethane, urethane+isoflurane and vehicle) were performed using one-way ANOVA. Post-hoc tests between two groups were performed with two-tailed unpaired t-test. A $p < 0.05$ is considered significant. These operations were performed using the AFNI software.

We also performed region-of-interest (ROI) analysis. ROIs were identified with the aid of a high-resolution coronal digital rat brain atlas (Paxinos and Watson, 2005) processed in MATLAB (The MathWorks, Inc., Natick, MA). MRI slice locations relative to bregma along the rostral-caudal direction were identified, and the digital atlas whose bregma coordinates matched the MRI slice locations were processed such that the matrix size and the format of those digital images were consistent with the MRI images. The dimensions of the digital atlas were linearly scaled in the X and Y directions so that the outer contour of individual digital images matched that of the MRI images. The processed digital atlas was saved in AFNI format. ROIs were then manually identified and drawn from the processed digital atlas. ME-MRI signal changes relative to pre-SMI baseline from all voxels within each ROI were averaged and compared between experimental groups using one-way ANOVA. Post-hoc comparisons were performed using the Tukey's tests. A $p <0.05$ is considered significant. These operations were performed using the SPSS software (SPSS Inc., Chicago, IL). Data are presented as mean ± standard error of the mean (SEM) unless otherwise specified.

Results

Evaluation of BBB Integrity Following Intravenous SMI-71 Using Evans Blue Dye Staining

To determine whether or not SMI-71 could disrupt rat BBB, we evaluated BBB integrity using the Evans blue staining method. Figure 1A shows whole brain pictures after SMI-71 and vehicle treatment, respectively. In vehicle-treated animal, blue stains appear only intravascular; but in animals receiving SMI-71 treatment, the blue stain diffuses throughout the brain parenchyma. Figures 1B and C illustrate 2 mm thick sections grossly dissected at similar locations from the above two animals. As indicated by the arrows, blue stain is distributed in both the cortical and subcortical structures in the SMI-71-treated animal. In contrast, there is minimal blue staining in the vehicle-treated animal except around blood vessels, which is probably an artifact of the dissection process. Notably, blue stain in caudate putamen (CPu) is deeper in color than in the neocortex, indicating more pronounced BBB disruption in CPu, which is consistent with our imaging results (see below).

ME-MRI Following Intravenous SMI-71

Following $MnCl_2$ infusion, we first observed signal enhancement in skull muscles due to the marked T_1 effect of Mn^{2+} in blood. About 5 min later, the ventricular signal started to increase. In contrast, signal changes within brain parenchyma were not observable until the BBB was disrupted by SMI-71. These observations are consistent with previous studies (Lin et al., 1997; Lu et al., 2007), presumably due to the fact that Mn^{2+} has limited permeability through the BBB (Fitsanakis, 2005). Of the three doses of SMI-71 employed (20, 25 and 30 μl), consistent BBB disruption was seen only in the high dose group (30 μl) and is reported here. Reducing SMI-71 infusion rate by doubling the infusion duration (from 5 min to 10 min) did not appear to affect the outcome. In all results described below, the infusion duration was fixed at 5 min. In general, we observed two distinct patterns of ME-MRI signal enhancement between the cortical and the subcortical structures. In the subcortical areas, such as CPu and nucleus accumbens (NAc), the amplitudes of ME-MRI were large (40%) and reached a plateau in about

30 min following SMI-71 infusion. In the neocortex, however, the amplitude of ME-MRI signal was typically <15%. As an example, figures 2A and B show group mean ME-MRI time courses in CPu and the barrel cortex (S1BF). The signal enhancement profiles in S1BF were similar in both the urethane and the urethane+isoflurane groups, although the magnitude and the slope of the enhancement were higher in the urethane alone group. However, the signal enhancement profiles in CPu were markedly different: for the urethane group, the ME-MRI signal was enhanced about 4 min following the initiation of anti-EBA agent infusion, reaching a plateau in about 10 min, while the signal enhancement in the urethane+isoflurane group was much slower in onset time and lasted a longer period of time. There were no significant signal changes pre- *vs.* post-vehicle infusions.

Statistical maps showing group main effects of ME-MRI signal change between the three groups (urethane, urethane+isoflurane and saline) are shown in figure 3 (top panel, one-way ANOVA, $F(2, 19) > 3.5$). There is significant signal enhancement inside the entire brain in animals receiving SMI-71. In both groups receiving SMI-71, ME-MRI signal enhancement was most prominent in subcortical structures, including CPu, NAc and hippocampus. Furthermore, in CPu, there is significantly more pronounced signal enhancement in the urethane+isoflurane group than the urethane group (Fig. 3 bottom panels, two-tailed unpaired t-test, $t > 2.2$).

Given the distinct cortical and subcortical signal enhancement patterns as shown in Fig. 3, we chose eight representative structures and defined ROIs based on the digital atlas. Figure 4 illustrates quantitative results from these ROIs. There are significant group effects within each ROI (one-way ANOVA, $F(2,19)> 9.2$). Two trends in ME-MRI signal were seen for the urethane alone and the urethane+isoflurane groups: the ME-MRI signal enhancement in the neocortex was greater in the urethane group; however, in the subcortical structures, there was an opposite trend, in particular, in CPu, there is significantly less signal enhancement in urethane group (post-hoc Tukey test, $p=0.04$)

From initial studies, it was clear that SMI-71 produced marked changes in mean arterial pressure (MAP). We recorded several physiological parameters including MAP and end-tidal CO_2 during the MRI scans. Typically, a significant increase in MAP developed approximately 2 min after the onset of SMI-71 administration, with peak values reaching ~210 mmHg in some animals, followed by an abrupt drop in MAP to 50~60 mmHg (Fig. 5). A MAP of 50-60 mmHg indicates a substantially compromised physiological condition. A previous ME-MRI study (Aoki et al., 2004) reported that the vasodilatory property of isoflurane was effective in reducing MAP associated with BBB disruption, we attempted to mitigate this problem by introducing isoflurane (see Methods). Isoflurane induces cerebral vasodilation and was effective in reducing the amplitude of the MAP increase after SMI-71 infusion, as shown in Fig. 5. More importantly, it also prevented the subsequent significant drop in MAP seen in the urethane alone group. The MAP value at the end of experiment was 126±44 mmHg (mean ± S.D.) in the urethane+isoflurane group, which is within normal cerebral blood flow autoregulation range (Guyton and Hall, 2000).

The increase in MAP appears to parallel the time course of ME-MRI signal enhancement within brain parenchyma. Figure 6 illustrates the relationship between changes in MAP and the degree of ME-MRI signal enhancement in six predefined ROIs. In general, there is a strong correlation between MAP increase and ME-MRI signal enhancement with the correlation coefficient > 0.8.

Once the BBB is disrupted, the duration that it remains open is an important factor for functional ME-MRI experimental design. To address this question, we performed continuous ME-MRI scanning while turning the $MnCl_2$ infusion pump on and off periodically, each infusion lasting

30 min. Since the half life of Mn^{2+} in blood in very short (Mendonça-Dias et al., 1983) and Mn^{2+} can readily enter the ventricles (Lu al., 2007), it can be expected that the signal intensity in ventricles would be modulated by Mn^{2+} concentration in blood; while the signal intensity in brain parenchyma will not change unless BBB remains open. Figure 7 shows ME-MRI signal in the ventricle and CPu. As expected, ME-MRI signal is modulated by the manganese infusion paradigm. More importantly, the signal in CPu is also modulated. Since the CPu signal would be expected to remain constant if BBB closes, such signal changes suggest that the BBB in CPu remains open for at least 2.5 hours, which is generally consistent with a previous study by Ghabriel et al. (2004) who reported BBB disruption for up to 2 hours with barrier restoration by 3 hours. These data suggest that there is approximately a 2.5 hour window to perform functional ME-MRI manipulations after BBB disruption using SMI-71.

Potential side effects resulting from both the SMI-71 agent and the vehicle are of a major concern. Pathological examination was performed on rat kidney, heart and lung tissues following about 2.5 hours of treatment (see methods, n=9). Sections of lung, heart and kidneys were reviewed for each rat. No lesions were identified in any of the tissues from any of the rats. There was no evidence of pulmonary edema in any of the rats (Dr. Michael A. Eckhaus, personal communications).

Discussion

Disruption of the BBB integrity is a prerequisite for acute imaging of the whole rat brain using Mn^{2+} as a contrast agent (Aoki et al., 2002; Lin and Koretsky, 1997; Lu et al., 2007). The traditional BBB opening method uses an intracarotid infusion of a hyperosmolar agent, which involves substantial surgical trauma and produces variable degrees of BBB disruption between animals. In the present study, we demonstrate an alternative approach: intravenous infusion of an anti-endothelial barrier antigen drug, which leads to BBB disruption of the whole brain. The procedure is simple and straightforward, avoiding many of the untoward effects related to intracarotid hyperosmotic stress and opens novel possibilities for dynamic ME-MRI experiments.

The degree of BBB opening as measured by fractional changes in the ME-MRI signal was heterogeneous across the rat brain, with more disruption in subcortical structures than neocortex (Figs. 3 and 4). The mechanism for this is unknown but may be related to a heterogeneous distribution in cerebral capillary density or EBA antigen density in these vessels. In most animals, infusion of SMI-71 resulted in a substantial increase in MAP, as shown in Fig. 5. Such changes in MAP correlated with BBB disruption. Although not systematically evaluated, in pilot non-imaging studies, we noticed that animals without an increase in MAP showed limited BBB disruption. We also noticed that some rats died immediately following SMI-71 infusion (with a nonsurvival rate of about 30%). Postmortem examination found a great amount of diffused Evans Blue dye into the lung tissue. Artificial ventilation significantly enhanced rat survival rate. In fact, there was not a single rat mortality using this procedure.

In this study, we attempted to minimize SMI-71 induced blood pressure changes using the gaseous anesthetic isoflurane (Fig 5). There was no difference in the effects of BBB opening to that with urethane anesthesia alone in NAc and amygdala, but was significantly more prominent in CPu. In contrast, the BBB opening in the neocortex appears less prominent when MAP was better maintained with isoflurane supplement (although not statistically significant). The benefit of such anesthetic manipulation was that MAP was maintained at a more normal level, helping to preserve a more or less normal physiological condition. The underlying mechanisms of differential BBB disruption under these two anesthetic regimes are unknown. In addition to the potential effects of anesthetics on the vascular walls, in particular the capillary endothelial cell membrane, the differential effects of the anesthetic agents on cardiac rate and

baseline blood pressure may be more important. In fact, it has long been recognized that cardiac dynamics is a significant mechanistic event in the opening of BBB. The study by Gumerlock et al. (1990) is of particular relevance. In that study, Sprague-Dawley rats were given pentobarbital, Ketamine-xylazine, methoxyflurane or fentanyl-droperidol before intracarotid infusion of mannitol or saline. They noted that rats anesthetized with methoxyflurane were more hypotensive than rats in other anesthetic groups and showed poor BBB opening. But increasing blood pressure to a normal level produced a barrier opening comparable to that of the other agents. They also showed that rats anesthetized with fentanyl-droperidol displayed significant tachycardia and poor BBB opening after mannitol infusion; slowing the cardiac rate with propranalol improved barrier opening.

Once disrupted, the BBB remains open for about 2.5 hours (Fig. 7), which is the suggested time window for task manipulations in functional ME-MRI experiments. Although not demonstrated here, one can imagine giving pharmacological challenges along with SMI-71 infusion. Alternatively, pharmacological challenges can be performed after the BBB is disrupted. The resulting ME-MRI signal enhancement would be the combined effects of BBB disruption and neuronal activation caused by pharmacological challenges, which can be differentiated by comparing ME-MRI signal enhancement between different treatment groups. Another strategy to separate the above two effects is to adjust Mn^{2+} infusion rate after BBB disruption so that a stable baseline can be reached and to perform pharmacological challenges later. It should also be noticed that BBB disruption is a major stressor, and has profound long-term brain effects such as the induction of an epileptic focus and neurodegeneration (Seiffert et al. 2004). It could also result in delayed functional and structural alterations in the rat neocortex (Tomkins et al. 2007). These pathological changes have to be considered when planning chronic studies and may limit the applicability of the proposed method to certain physiological questions. However, it might be interesting to use ME-MRI to study the pathological sequence of BBB disruption itself.

Technical Considerations

Our choice of urethane for the current ME-MRI study was based on pilot experiments using Evans blue dye as the indicator of BBB integrity. Given the nature of such experiments, we only had a single time window to examine the distribution of the dye, which was 10 min after SMI-71 was infused (see Methods). ME-MRI scans offer the opportunity to examine the dynamic process of BBB disruption across the entire rat brain. We found that the process of BBB disruption was different in animals receiving isoflurane compared with those receiving urethane alone, as shown in Fig. 1. These data suggest that by using Evans blue dye to examine the outcome of BBB disruption, we might have missed the optimum time window for other anesthetic agents. Urethane is carcinogenic and cannot be applied in survival experiments. Given that anesthetic agents can differentially affect BBB opening outcome as discussed above, it would be of interest to search for a more appropriate anesthetic agent for longitudinal ME-MRI experiments using SMI-71.

In summary, we have demonstrated that intravenous infusion of the anti-EBA agent SMI-71 leads to whole brain BBB disruption as detected by ME-MRI. The procedure is simple and straightforward and opens novel possibilities for functional neuroimaging using the ME-MRI technique, including the possibility of within subject design studies. However, it should also be noted that neither the anti-EBA agent nor the vehicle was tested for sterility, toxicity or pyrogenicity, thus its applicability for chronic long term experiments is as yet unknown.

Acknowledgments

We would like to thank Michael A. Eckhaus, V.M.D, chief of Pathology Service at the Division of Veterinary Resources, ORS, OD, National Institutes of Health for performing pathological examinations; we would also like to

thank Drs. Marisela Morales and Hui Shen for technical support in histological preparation and Thomas J. Ross for discussions on statistical analysis. This work was supported by the Intramural Research Program of the National Institute on Drug Abuse, National Institutes of Health.

References

Aoki I, Tanaka C, Takegami T, Ebisu T, Umeda M, Fukunaga M, Fukuda K, Silva AC, Koretsky AP, Naruse S. Dynamic activity-induced manganese-dependent contrast magnetic resonance imaging (DAIM MRI). Magn Reson Med 2002;48:927–933. [PubMed: 12465100]

Aoki I, Naruse S, Tanaka C. Manganese-enhanced magnetic resonance imaging (MEMRI) of brain activity and applications to early detection of brain ischemia. NMR Biomed 2004;17:569–580. [PubMed: 15617055]

Beck DW, Hart MN, Hansen KE. Effect of intracarotid hyperosmolar mannitol on cerebral cortical arterioles--a morphometric study. Stroke 1984;15:134–136. [PubMed: 6420944]

Canals S, Beyerlein M, Keller AL, Murayama Y, Logothetis NK. Magnetic resonance imaging of cortical connectivity in vivo. Neuroimage 2008;40:458–472. [PubMed: 18222710]

Cox RW. AFNI: software for analysis and visualization of functional magnetic resonance neuroimages. Comput Biomed Res 1996;29:162–173. [PubMed: 8812068]

Duong TQ, Silva AC, Lee SP, Kim SG. Functional MRI of calcium-dependent synaptic activity: cross correlation with CBF and BOLD measurements. Magn Reson Med 2000;43:383–392. [PubMed: 10725881]

Fitsanakis VA, Piccola G, Aschner JL, Aschner M. Manganese transport by rat brain endothelial (RBE4) cell-based transwell model in the presence of astrocyte conditioned media. J Neurosci Res 2005;81:235–243. [PubMed: 15948148]

Ghabriel MN, Lu JJ, Tadros R, Hermanis G. A narrow time-window for access to the brain by exogenous protein after immunological targeting of a blood–brain barrier antigen. J Comp Path 2004;131:52–60. [PubMed: 15144799]

Ghabriel MN, Zhu C, Hermanis G, Allt G. Immunological targeting of the endothelial barrier antigen (EBA) in vivo leads to opening of the blood-brain barrier. Brain Res 2000;878:127–135. [PubMed: 10996143]

Gumerlock MK, Neuwelt EA. The effects of anesthesia on osmotic blood-brain barrier disruption. Neurosurgery 1990;26:268–277. [PubMed: 2308675]

Guyton, AC.; Hall, JE. Textbook of Medical Physiology. 10th. W. B. Saunders Company; Philadelphia, USA: 2000.

Hsu YH, Chen CC, Zechariah A, Yen CC, Yang LC, Chang C. Neuronal dysfunction of a long projecting multisynaptic pathway in response to methamphetamine using manganese-enhanced MRI. Psychopharmacology 2008;196:543–553. [PubMed: 18000655]

Jensen NF, Todd MM, Kramer DJ, Leonard PA, Warner DS. A comparison of the vasodilating effects of halothane and isoflurane on the isolated rabbit basilar artery with and without intact endothelium. Anesthesiology 1992;76:624–634. [PubMed: 1550288]

Kolb B, Whishaw IQ. Fundamental of Human Neuropschology 2003:119–120.

Kuo YT, Herlihy AH, So PW, Bell JD. Manganese-enhanced magnetic resonance imaging (MEMRI) without compromise of the blood-brain barrier detects hypothalamic neuronal activity in vivo. NMR Biomed 2006;19:1028–1034. [PubMed: 16845705]

Lin YJ, Koretsky AP. Manganese ion enhances T1-weighted MRI during brain activation: an approach to direct imaging of brain function. Magn Reson Med 1997;38:378–388. [PubMed: 9339438]

Lu H, Yang S, Zuo Y, Demny S, Stein EA, Yang Y. Real-time animal functional magnetic resonance imaging and its application to neuropharmacological studies. Magn Reson Imaging 2008;26:1266–1272. [PubMed: 18448300]

Lu H, Xi ZX, Gitajn L, Rea W, Yang Y, Stein EA. Cocaineinduced brain activation detected by dynamic manganese-enhanced magnetic resonance imaging (MEMRI). Proc Natl Acad Sci USA 2007;104:2489–2494. [PubMed: 17287361]

Lu H, Demny S, Rea W, Zuo Y, Yang Y, Stein EA. A novel method for dynamic manganese-enhanced MRI. Proc Intl Soc Magn Reson Med 2009;17:153.

Mendonça-Dias MH, Gaggelli E, Lauterbur PC. Paramagnetic contrast agents in nuclear magnetic resonance medical imaging. Semin Nucl Med 1983;13:364–376. [PubMed: 6359418]

Paxinos, G.; Watson, C. The Rat Nernous System. 5th. Academic Press Inc.; San Diego: 2005.

Pautler RG, Silva AC, Koretsky AP. In vivo neuronal tract tracing using manganese-enhanced magnetic resonance imaging. Magn Reson Med 1998;40:740–748. [PubMed: 9797158]

Pautler RG, Koretsky AP. Tracing odor-induced activation in the olfactory bulbs of mice using manganese-enhanced magnetic resonance imaging. Neuroimage 2002;16:441–448. [PubMed: 12030829]

Seiffert E, Dreier JP, Ivens S, Bechmann I, Tomkins O, Heinemann U, Friedman A. Lasting blood-brain barrier disruption induces epileptic focus in the rat somatosensory cortex. J Neurosci 2004;24:7829–7836. [PubMed: 15356194]

Sternberger NH, Sternberger LA. Blood-brain barrier protein recognized by monoclonal antibody. Proc Natl Acad Sci USA 1987;84:8169–8173. [PubMed: 3500474]

Tomkins O, Friedman O, Ivens S, Reiffurth C, Major S, Dreier JP, Heinemann U, Friedman A. Blood-brain barrier disruption results in delayed functional and structural alterations in the rat neocortex. Neurobiol Dis 2007;25:367–377. [PubMed: 17188501]

Watanabe T, Radulovic J, Boretius S, Frahm J, Michaelis T. Mapping of the habenulo-interpeduncular pathway in living mice using manganese-enhanced 3D MRI. Magn Reson Imaging 2006;24:209–215. [PubMed: 16563949]

Wolman M, Klatzo I, Chui E, Wilmes F, Nishimoto K, Fujiwara K, Spatz M. Evaluation of the dyeprotein tracers in pathophysiology of the blood-brain barrier. Acta Neuropathol 1981;54:55–61. [PubMed: 7234328]

Yu X, Wadghiri YZ, Sanes DH, Turnbull DH. In vivo auditory brain mapping in mice with Mn-enhanced MRI. Nat Neurosci 2005;8:961–968. [PubMed: 15924136]

Yu X, Sanes DH, Aristizabal O, Wadghiri YZ, Turnbull DH. Large-scale reorganization of the tonotopic map in mouse auditory midbrain revealed by MRI. Proc Natl Acad Sci USA 2007;104:12193–12198. [PubMed: 17620614]

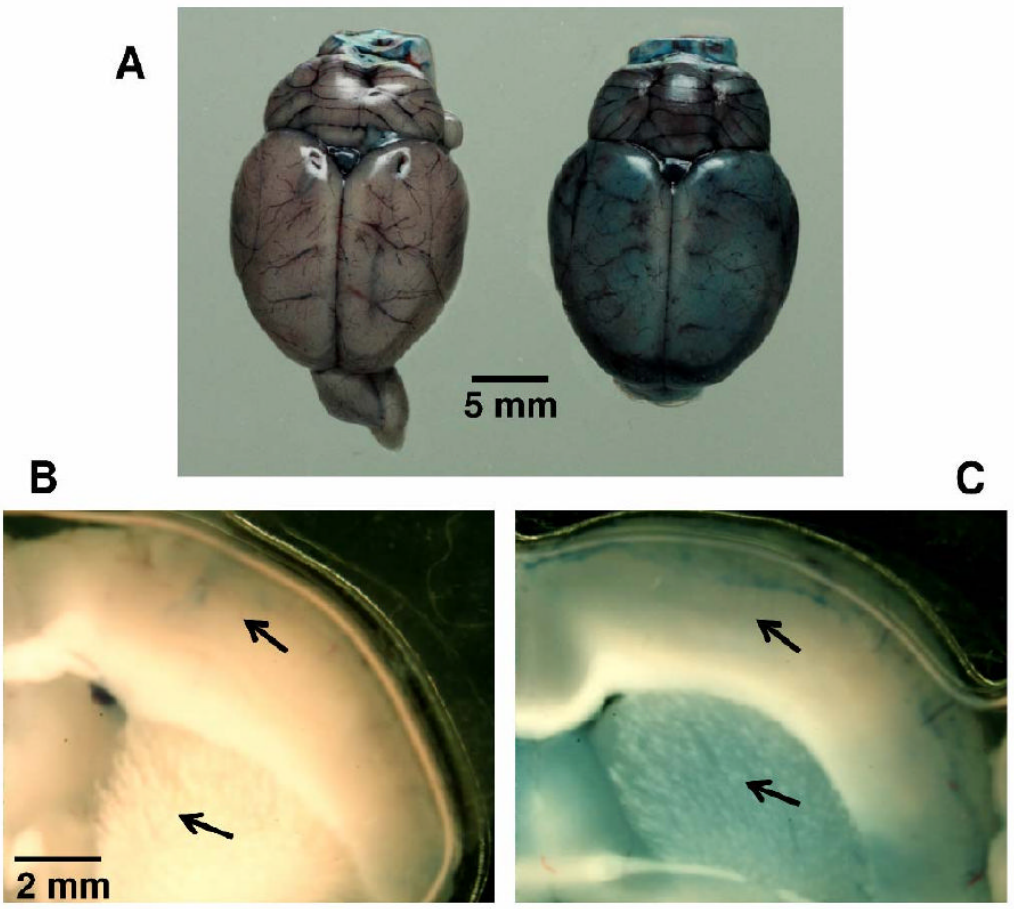

Figure 1.

The effects of SMI-71 on the integrity of rat blood-brain barrier assessed with Evans blue dye. Note the diffusive distribution of Evans blue dye in SMI-71-treated rat brain (*A*, right). But the blue stains appear only inside vessels in vehicle-treated rat animal (*A*, left). *B* and *C* show Evans blue distributions in sections grossly dissected (2 mm in thickness) at similar locations. As indicated by the arrows, blue stains are distributed in both the cortical and subcortical structures in SMI-71-treated animal (*C*); there are minimal blue stains in the vehicle-treated animal (*B*) except some stains around vessels.

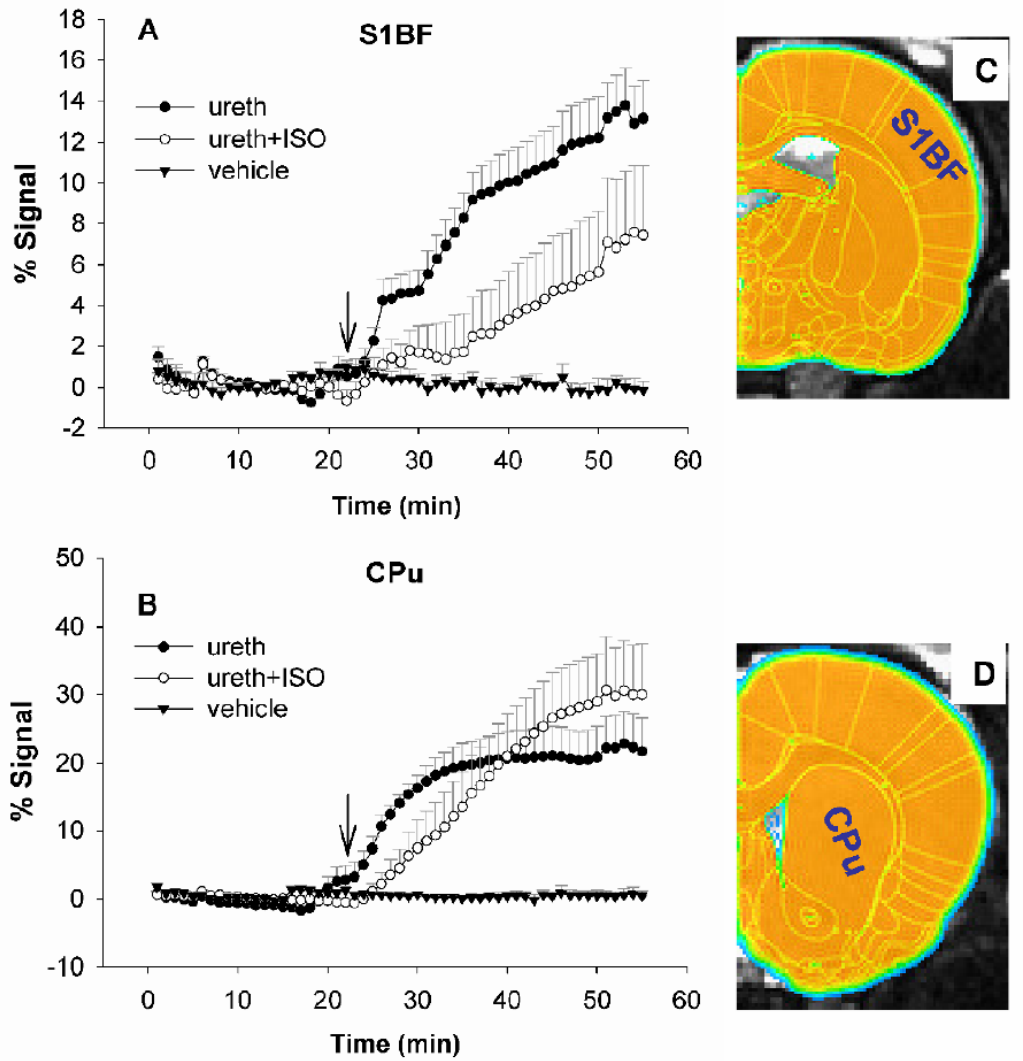

Figure 2.

Mean signal time courses from the primary somatosensory cortex of the barrel field (S1BF, 168 voxels) and caudate putamen (CPu, 346 voxels) in three experimental groups. Note different signal enhancement profiles between rats under urethane anesthesia alone (***A***: Ureth, n=10) and those under urethane+isoflurane (***B***: Ureth+ISO, n=6). There was no significant signal enhancement following vehicle injection. ROIs were identified by overlaying a digital rat brain atlas onto T_2-weighted anatomical images, as shown in ***C*** and ***D***. S1BF and CPu are marked on half of the hemisphere for graphic clarity; voxels from bilateral ROIs are included for calculation. Arrows indicate the initiation of intravenous infusion of SMI-71 or vehicle.

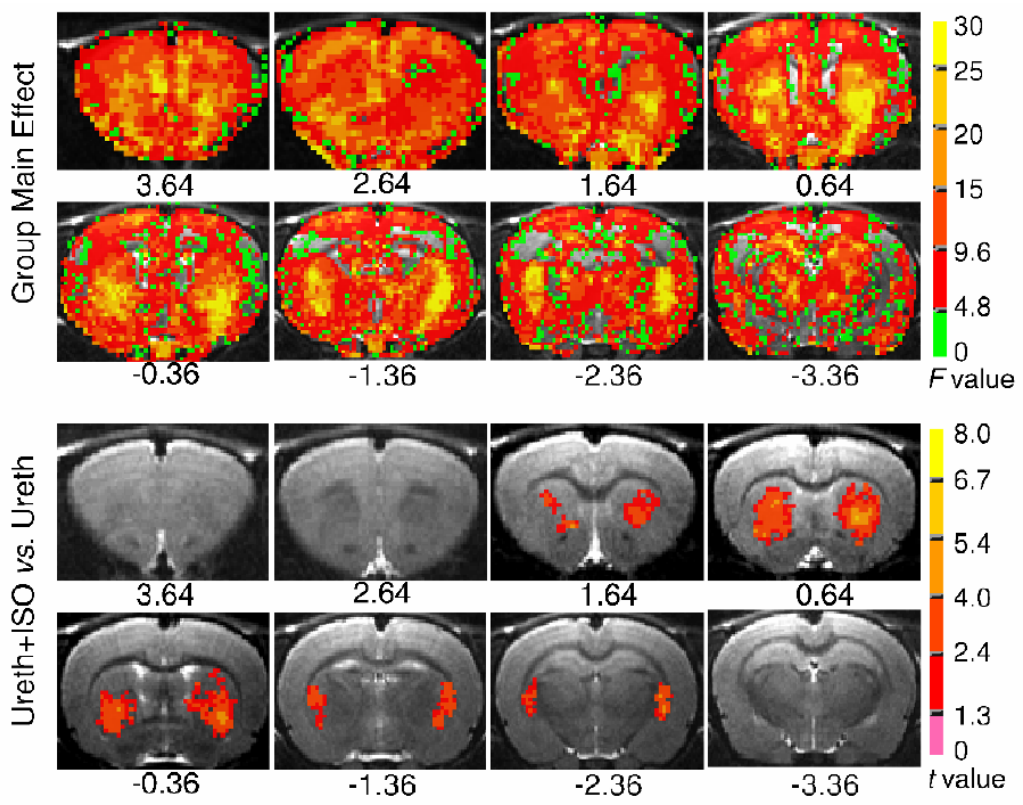

Figure 3.

Top panels: pseudo color maps showing the group main effects of ME-MRI signal enhancement (one-way ANOVA, $F(2,19)>3.5$, $p<0.05$) following intravenous infusion of SMI-71 (n=10 for the urethane group; n=6 for urethane+isoflurane group) or vehicle (n=6). Of the two groups receiving SMI-71 treatment, the effects of BBB disruption were similar in most structures except in caudate putamen (bottom panels, two-tailed unpaired t-test, $t>2.2$, $p<0.05$). Numbers below images are coordinates relative to bregma. Color bars show *F* and t values, respectively.

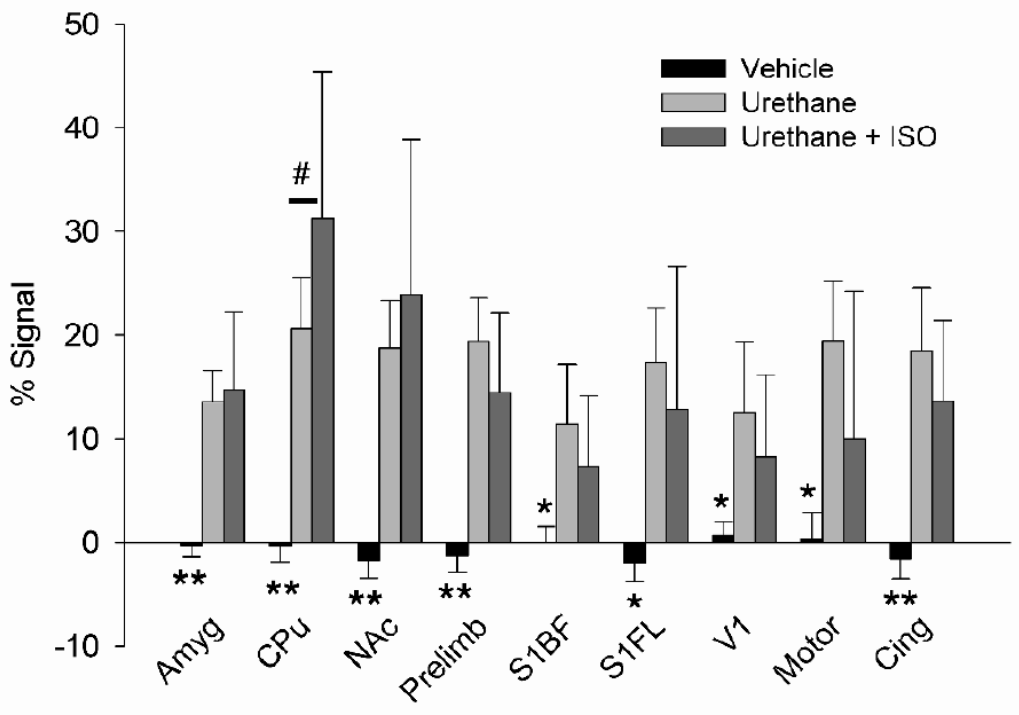

Figure 4.

ME-MRI signal intensity changes following intravenous infusion of vehicle or SMI-71 in animals under urethane anesthesia alone (Ureth) or under urethane+isoflurane (Ureth+ISO). The ROIs were identified in a similar fashion as shown in Fig. 1. Group main effects were compared using one-way ANOVA (**, $F(2,19)>16$, $p<0.0001$; *, $F(2,19)>9$, $p<0.002$. Post-hoc Tukey analyses indicate signal enhancement in CPu is significantly reduced in the Ureth group vs. the Ureth+ISO group (#, $p=0.04$). Abbreviations: Amyg, amygdala; Cing, cingulate cortex; CPu, caudate putamen; NAc, nucleus accumbens; Prelimb, pre-limbic cortex; S1BF, primary somatosensory cortex of the barrel field; V1 primary visual cortex; Motor, motor cortex.

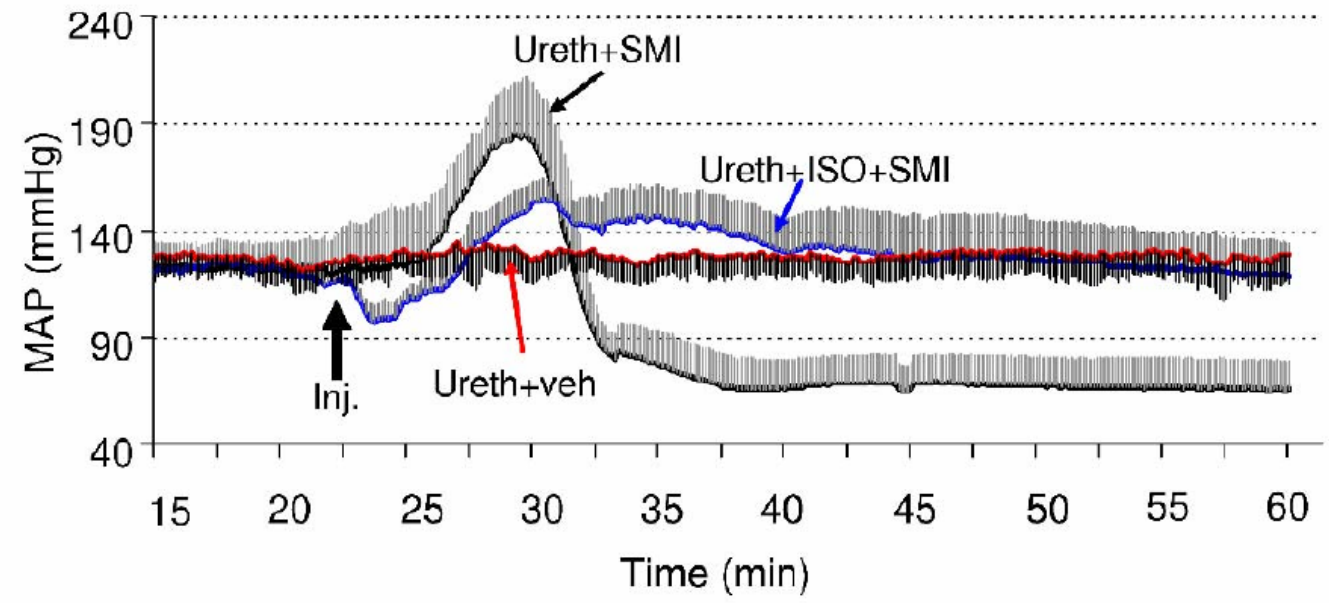

Figure 5.
Mean arterial pressure (MAP) changes following intravenous infusion of vehicle or SMI-71 (indicated by the bold black arrow) in animals under urethane anesthesia alone (Ureth) or under urethane+isoflurane (Ureth+ISO). Data represent mean ± SEM. MAP values during other time periods were not shown for graphic clarity.

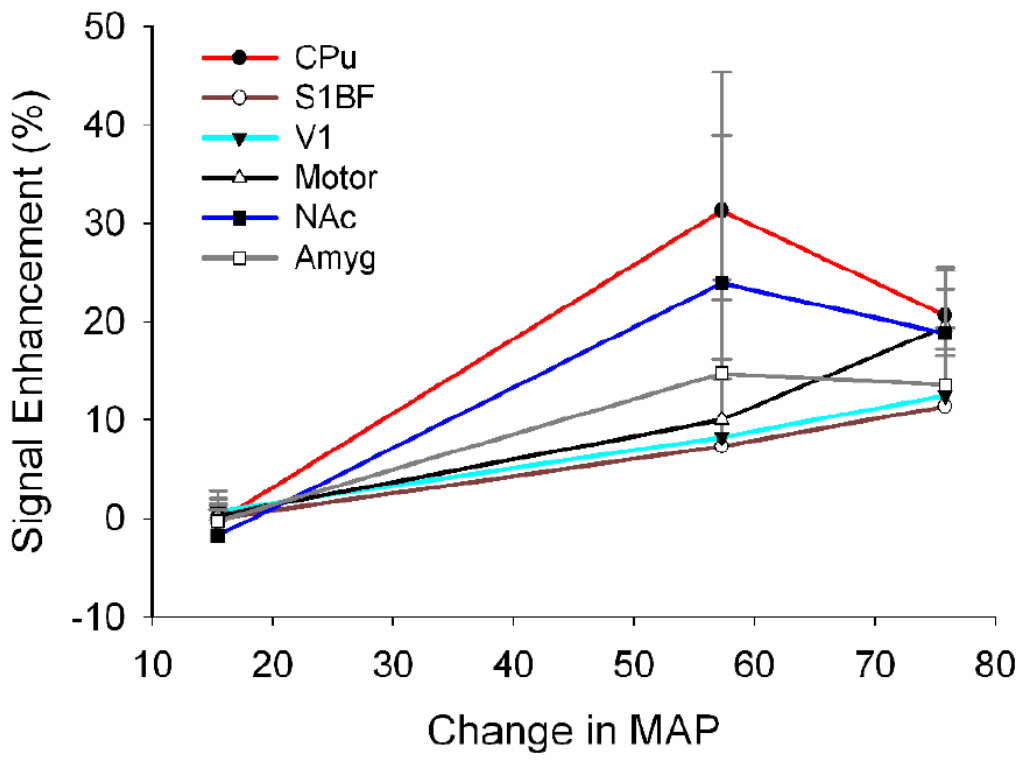

Figure 6.
The relationship between ME-MRI signal enhancement and increase in mean arterial blood pressure (peak values). The degree of BBB disruption as measured by ME-MRI signal enhancement in six cortical and subcortical structures is correlated with mean arterial blood pressure increase with the correlation coefficients > 0.8. Abbreviations are the same as in Fig. 4.

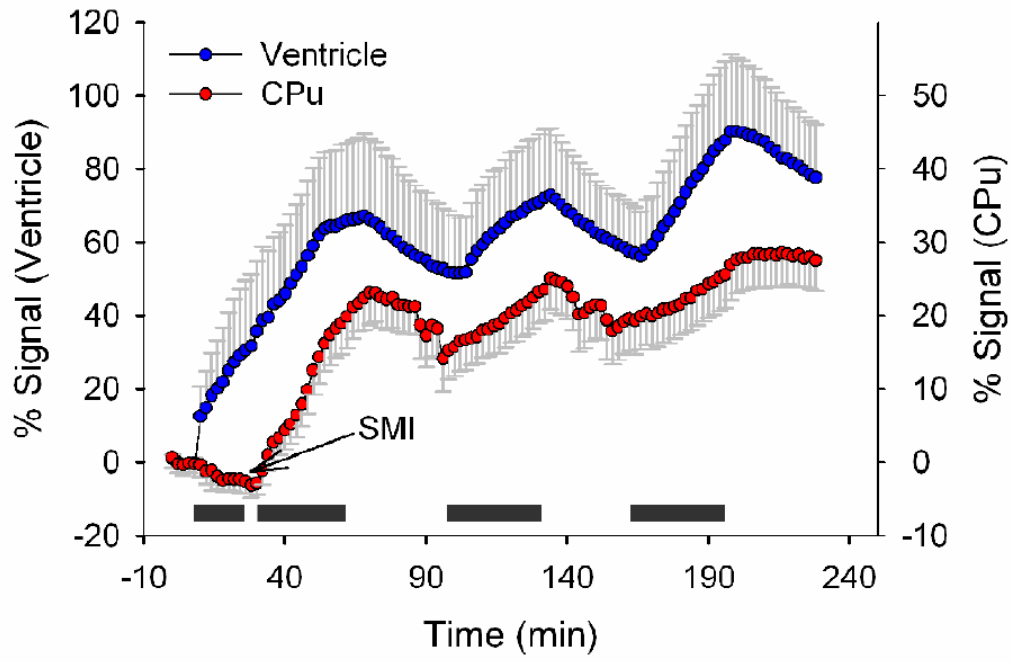

Figure 7.

Averaged time courses showing ME-MRI signal modulated by manganese infusion paradigm from one animal (caudate putamen (CPu), 346 voxels; ventricles, 68 voxels). Grey bars indicate the periods of manganese infusion. Since manganese can readily enter ventricles, the ventricle curve reflects Mn^{2+} concentration in blood as modulated by manganese infusion; while ME-MRI signal variations in CPu suggest that BBB remains open for about 2.5 hours following SMI-71 infusion.